# Microstructural evolution of TiC/near-α Ti composite during high-temperature tensile test

J.Q. Qi, J. Lu, Y.Z. He, Y.W. Sui,[a] Q.K. Meng, and F.X. Wei
*School of Materials Science and Engineering, China University of Mining and Technology, Xuzhou 221116, People's Republic of China*

Z.J. Wei
*School of Materials Science and Engineering, Harbin Institute of Technology, Harbin 150001, People's Republic of China*

(Received 22 June 2016; accepted 13 September 2016)

In the present paper, 10 vol%TiC/Ti–6Al–3Sn–3.5Zr–0.4Mo–0.75Nb–0.35Si composite produced via in situ casting technique was tested in the temperature range from room temperature to 900 °C and much attention was paid on the microstructural evolution during high-temperature tensile test. It was found that the variation of microstructures in deformation zones with strain exhibited different trends at different temperatures. Below 600 °C, dislocation density increased with strain over the entire strain range. As temperature increased to 700 °C, dislocations proliferated rapidly in the initial deformation and then dislocation annihilated through dynamic recovery. Above 800 °C, the variation of microstructures in deformation zones with strain was similar to that at 700 °C at the beginning but at higher strain, dynamic recrystallization (DRX) occurred, leading to the formation of equiaxed microstructure. Microstructural evolution in deformation zones corresponded to the variation of tensile stress–strain characteristics with temperature, reflecting the hardening or softening feature of matrix. Dynamic recovery ascribed to the flow softening of the composite at 700 °C, while flow softening is owing to dynamic recovery and DRX above 800 °C. In addition, matrix softening should show different trends in different temperature ranges.

## I. INTRODUCTION

Metal matrix composites (MMCs), acting as an important type of metal, have been designed and developed in the past several decades, which offer a combination of the ductility of metal and strength and hardness of reinforcement.[1–4] As a typical member of MMCs family, discontinuously reinforced titanium matrix composites (DRTMCs) have been considered as the optimal candidate materials for aerospace application due to their high strength-to-weight ratio, good corrosion/oxidation resistance, high strength, and excellent creep resistance at high temperatures.[5–8] In situ technique has been widely used to fabricate DRTMCs, which mainly includes powder metallurgy (PM)[9,10] and combustion assisted cast.[11,12] Compared to PM technique, the latter can produce large-scale DRTMC castings with high compactness and low cost, which has attracted more and more attention.[13–15] In DRTMCs, TiC particles have been proved to be one of the most suitable reinforcements because of their good properties and excellent compatibility with titanium matrices.[16–19]

High-temperature tensile test has been performed on DRTMCs to understand the dependence of tensile properties on temperature and microsturcture.[20–22] It is well established that the tensile strengths of DRTMCs decrease gradually with the increase of temperature, whereas the ductility shows an opposite trend.[21] Much work pointed out that matrix softening plays a dominant role in the degradation of tensile strengths of DRTMCs.[23] Badini et al.[24] indicated that the tensile strength of 10 vol%TiC/Ti–6Al–4V composite displays almost linear decrease in the temperature range from room temperature to 800 °C, meaning that matrix softening becomes more and more serious with increasing temperature. However, little work has been conducted on the matrix softening feature of DRTMCs as high-temperature titanium alloy was selected as matrix.

Hot deformation behaviors of titanium alloys and DRTMCs have been widely investigated with cylindrical specimens through isothermal compression.[25,26] During hot deformation, the mechanisms of flow softening were reported to be dynamic recovery and dynamic recrystallization (DRX).[27,28] Flow softening was also found in DRTMCs during high-temperature tensile test, which constrains the further increase of tensile strengths.[5,22] Investigating on microstructure evolution is helpful for the understanding of flow softening behavior and the microstructure control of DRTMCs in this process.

Contributing Editor: Jürgen Eckert
[a]Address all correspondence to this author.
e-mail: wyds123456@outlook.com
DOI: 10.1557/jmr.2016.359

https://doi.org/10.1557/jmr.2016.359 Published online by Cambridge University Press

 © Materials Research Society 2016

However, few published reports have been performed on this kind of research.

In this work, 10 vol%TiC/Ti–6Al–3Sn–3.5Zr–0.4Mo–0.75Nb–0.35Si composite produced via in situ technique was tested at various temperatures. The main objective is to investigate the microstructural evolution and softening behavior of the composite during high-temperature tensile test.

## II. EXPERIMENTAL PROCEDURE

In this experiment, 10 vol%TiC/Ti–6Al–3Sn–3.5Zr–0.4Mo–0.75Nb–0.35Si composite was prepared by in situ casting technique and the detailed procedure was described in our previous work.[29] After casting, the composite casting was cut by electric discharging for microstructural observation and tensile test.

The microstructures were carried out using optical microscopy, and FEI Tecnai $G^2$ F30 transmission electron microscopy (TEM; FEI Company, Hillsboro, Oregon). The TEM specimens with 50 μm thickness were prepared by ion-beam thinning and twin-jet electropolishing. Flat tensile specimens with a gauge length of 20 mm and cross section of 4 mm × 2 mm were used for tensile test. Tensile test was conducted on Instron 5500R testing machine (Instron, Canton, Massachusetts) at the strain rate of 0.5 mm/min at room temperature, 200, 300, 400, 600, 700, 800, and 900 °C. At each temperature, at least three specimens were repeated and tensile strengths listed in this paper are average values.

To investigate the microstructure variation in deformation zones at high temperatures, tensile termination experiment was performed on the composite. This type of experiment can be described as follows: when the deformation amount reached needed value, tensile test was terminated and the tensile specimens were quenched in water immediately. Then, microstructures in deformation zones were observed using TEM. It should be noted that TEM specimens were cut from the middle of unbroken tensile samples or from the position just below the fracture surfaces of fractured samples.

## III. RESULTS AND DISCUSSION

### A. Phase identification and microstructure

Figure 1 displays the x-ray diffraction pattern of the as-prepared composite. The diffraction peaks can be indexed to TiC and α-Ti phases, indicating that TiC reinforced titanium alloy composite was fabricated.

Figure 2 shows the microstructure of the as-prepared composite. TiC mainly grew in equiaxed or near-equiaxed shape with size of 1–10 μm and some extent of particle clustering on a microscopic scale can be observed.[29] α phase in some regions without TiC particles displayed lamellar structure with colony characteristic, whereas α phase in TiC clusters grew in equiaxed or near-equiaxed morphology after the solid transformation of β → α. Previous work indicated that the growth of α phase in TiC segregation areas can be impeded, resulting in the formation of equiaxed or near-equiaxed α phase in these areas.[30,31] The width of α phase varied from 2 μm to 18 μm.

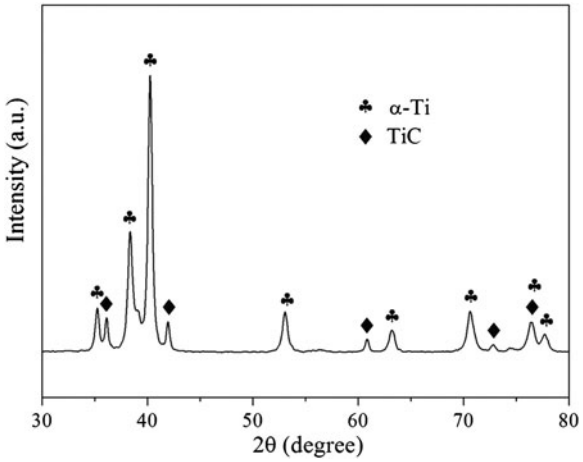



FIG. 1. X-ray diffraction pattern of the composite.

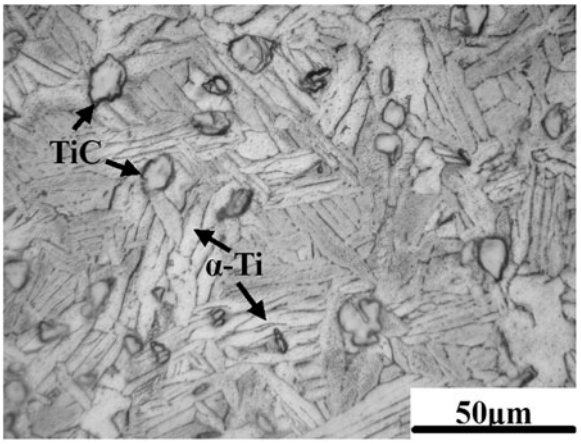



FIG. 2. Optical micrograph of the as-prepared composite.

### B. High-temperature stress–strain characteristic

Figure 3 illustrates the variation of ultimate tensile strength (UTS) of the composite with testing temperature in the form of average value ± standard deviation. Overall, tensile strength decreases with increasing temperature. However, the decrease of UTS shows different trends in different temperature ranges. In the temperature range from room temperature to 600 °C, UTS decreases slowly, whereas above 600 °C, fast degradation in UTS is observed. As we know, the decrease in tensile strength is mainly attributed to matrix softening. Hence, matrix softening trends in different temperature ranges are also different. Below 600 °C, matrix was softened slowly with increasing temperature. However, matrix softening

https://doi.org/10.1557/jmr.2016.359 Published online by Cambridge University Press

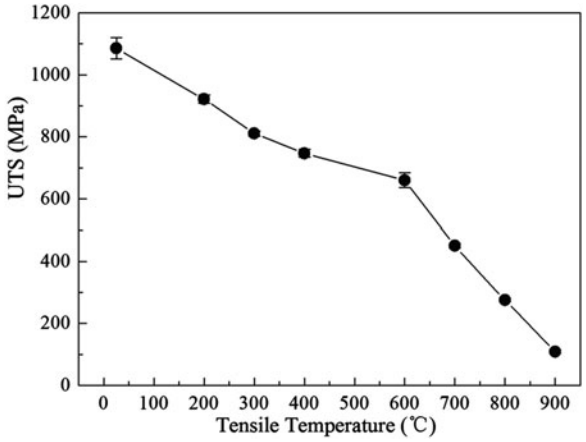



FIG. 3. The UTS of the composite as a function of testing temperature.

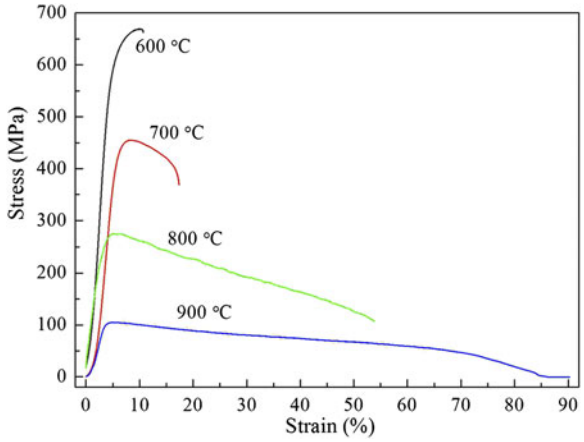



FIG. 4. High-temperature tensile stress–true strain curves of the composite.

becomes more and more serious from 600 °C to 900 °C. This type of variation reflects the characteristic of the composite to a large extent.

It has been reported that the understanding of stress–strain characteristic of the composite at high temperatures can provide useful insight into matrix softening behavior.[32] Figure 4 displays the tensile stress–strain curves of the composite at high temperatures. It can be observed that at 600 °C, after macroscopic yielding, the tensile stress of the composite increases with increasing strain. That is to say, tensile strength is higher than yield strength, equal to fracture strength. Similar feature of tensile stress–strain curves at high temperatures in DRTMCs were obtained.[33] As testing temperature is beyond 700 °C, some different features in tensile stress–strain curves can be seen (Fig. 4). After yielding, tensile stress reaches to its maximum at small strain, i.e., tensile strength is very close to yield strength and with further increase in strain, tensile stress decreases gradually. Liu et al.[22] obtained similar tensile stress–strain curves in TiC particle-reinforced titanium matrix composite at high temperature.

It is also observed that when tensile stress approaches to peak, the corresponding strain obtained from stress–strain curve decreases with temperature, which are 6.5%, 4.8%, and 3.4% at 700 °C, 800 °C, and 900 °C, respectively. Obviously, with the increase of temperature, the yielding of the composite occurs at lower strain. That is to say, the composite is more prone to yield at higher temperature, which is in accordance with matrix softening characteristic of the composite.

### C. Microstructural evolution in deformation zones

Based on the results in Fig. 4, as plastic deformation occurs, there exist obvious differences in the variation of stress with strain at different temperatures. The stress decreases faster with increasing plastic strain at 700 °C compared to that at 800 °C and 900 °C. This feature reflects that the discrepancy in the microstructure evolution with strain at different temperatures should exist. So, it is necessary to investigate the microstructures in deformation zones at different strains and different temperatures. Considering that TiC particles can not be deformed in the temperature range, the deformation amount of the composite depends on the deformability of matrix and the deformation mode of matrix can represent that of the composite.[29] Thus, much attention has been paid on the evolution of matrix microstructure with strain and temperature.

After the composite fractured at 600 °C, the TEM microstructure in deformation zone is shown in Fig. 5. As TEM specimen of the failed composite tested at 600 °C was ion-beam thinned, fractured TiC particle can be seen clearly but dislocation can not be found at the interface between TiC and matrix or in the interior of matrix [Fig. 5(a)] [The selected area diffraction patterns of TiC and α-Ti are shown in Figs. 5(b) and 5(c), respectively]. The dislocation should exist since the composite was plastically deformed. Dislocation may disappear during ion-beam thinning. So, twin-jet electropolishing was used to fabricate the TEM specimen. It can be seen that high density of dislocation not only can pile up at the interfaces between two α laths [Fig. 5(d)], but also can tangle in α-Ti phase [Fig. 5(e)]. The intersection of dislocations induced by dislocation motion from different directions will become obstacles and impede the subsequent dislocation motion, resulting in the formation of dislocation entanglement. This kind of entanglement will further hinder the motion of dislocation and thus be conducive to the work hardening of the composite. Therefore, the tensile stress increases with the increase in strain at 600 °C. It is reasonable to believe that at lower temperatures, the evolution of tensile stress with strain should be similar to that at 600 °C.

Liu et al.[34] indicated that the reinforcements in titanium matrix composites not only can enhance

https://doi.org/10.1557/jmr.2016.359 Published online by Cambridge University Press

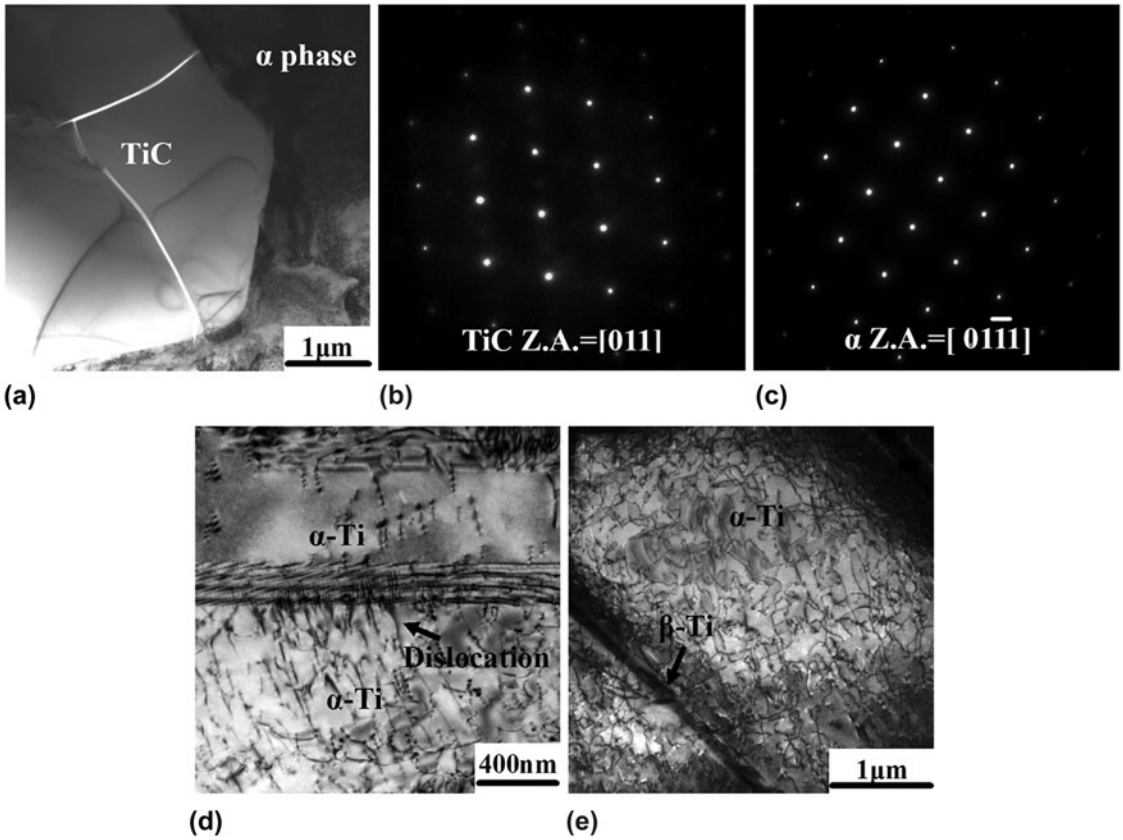



FIG. 5. TEM microstructure in deformation zone of the composite tested at 600 °C: (a) fractured TiC, (b) selected area diffraction pattern of TiC in (a), (c) selected area diffraction patterns of α-Ti in (a), (d) dislocation at α/α interface, and (e) dislocation within α phase.

mechanical properties and refine the matrix but also induce the plastic instability during hot deformation process. TiC particles can impede the movement of dislocations during high-temperature tensile test and accordingly, high-density dislocations will be generated at the particle/matrix interface, which is confirmed in Fig. 5. This is an important reason why composites show high stress level.

Figure 6 shows the microstructures in deformation zones of the composite with different strains at 700 °C. It is clearly observed from the TEM micrographs that the microstructures in deformation zones change with strain significantly. As tensile stress reaches to its peak (the corresponding strain is about 6% and the composite experienced a small amount of plastic deformation), entangled dislocation with high density was formed [Fig. 6(a)]. Although the plastic deformation of composite is very small, there are still a large number of dislocations. Apparently, the generation of dislocation is very sensitive to the plastic deformation.

As strain approaches to about 12%, the dislocation density in deformation zone decreased significantly, and dislocation arrangement becomes more regular [Fig. 6(b)]. At higher magnification, regular dislocation wall can be observed [Fig. 6(c)]. High density of dislocation generated at the initial strain results in high distortional energy stored in the matrix of the composite, so that the material is in an unstable state in thermodynamics. When hot deformation was performed on the specimen, dynamic recovery would occur through dislocation climbing and as a result, the dislocation with high-energy state and disorderly arrangement can be transferred into regular dislocation walls. These dislocation walls consisted of low-angle sub-boundaries, which provide the condition for the formation of recovered subgrains [Figs. 6(b) and 6(c)].

With further increase in strain, dislocation tangles almost disappeared and the dislocation in matrix is in regular arrangement state, as shown in Fig. 6(d). Evidently, the dislocation annihilation rate is higher than its formation rate. Furthermore, the typical subgrains were formed in deformation zone and the sub-boundaries consisted of dislocation network [Fig. 6(d)], which present typical dynamic recovery feature. These results suggests that strain has significant effect on microstructure.

According to microstructure evolution in deformation zone of the composite at 700 °C, it is easily obtained that the main flow softening mechanism is dynamic recovery. Just because of this, strain hardening induced by the

https://doi.org/10.1557/jmr.2016.359 Published online by Cambridge University Press

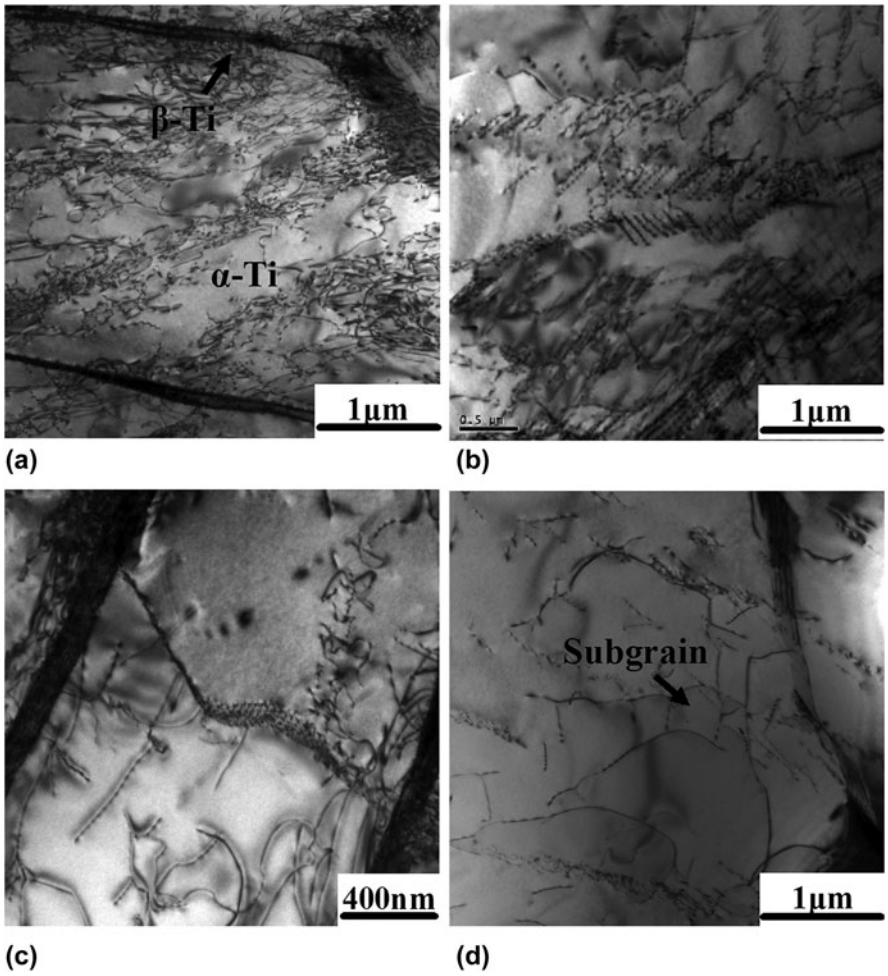



FIG. 6. Variation of matrix features in deformation zones of the composite with strain of (a) about 6%, (b) (c) 12%, and (d) 18% (fracture strain) at 700 °C.

formation of new dislocations can be offset by dynamic recovery and thus, the composite can not be strengthened further through plastic deformation. The competitions between the strain hardening and softening result in the formation of flowing stress–strain curve at 700 °C in. Usually, dynamic recovery dominates the flow softening process at low temperatures.[35,36]

As testing temperature increased to 800 °C, structure evolution in deformation zone is shown in Fig. 7. At strain of about 5%, high density of dislocation with dislocation loop was generated in matrix [Fig. 7(a)], which is similar to that found in the composite experiencing a similar strain at 700 °C [Fig. 6(a)]. This means that dislocation multiplication happened at the initial strain even though testing temperature increased to 800 °C. In addition, dislocation loops resulting from the vacancy collapse were observed in Fig. 7(a), which were reported in another work.[37] Further increase in strain (about 30%) led to the formation of cellular substructure, as shown in Fig. 7(b), which resulted from dislocation motion during dynamic recovery. At strain of about 43% (fracture strain), α lamellar was globularized markedly, as illustrated in Fig. 7(c). Undoubtedly, strain induces the transformation of lamellar structure to homogeneous globular one at 800 °C. The formation of equiaxed microstructure is attributed to DRX.[38,39]

The reinforcements in DRTMCs should have some role on DRX during thermomechanical processing. Humphreys and Hatherly[40] indicated that at high strain, the accumulation of dislocations is usually related to local lattice rotations in the regions near the particles and these regions are often called particle deformation zones (PDZs). High-density dislocations in PDZs provide high driving force for recrystallization and thus promote the refinement of grains in these regions. Wang et al.[41] also pointed out that globularization of elongated α phase and DRX of prior β grains occur prior near $TiB_w$ region owing to high-density dislocation in this region and the role of heterogeneous nucleation of $TiB_w$ on DRX in $TiB_w$/Ti60 composite during hot deformation. Our previous work confirmed that TiC particles can serve as effective heterogeneous nucleation substrates for α phase in titanium matrix composites.[12] It was also reported that micron-sized particles in hot-deformed

https://doi.org/10.1557/jmr.2016.359 Published online by Cambridge University Press

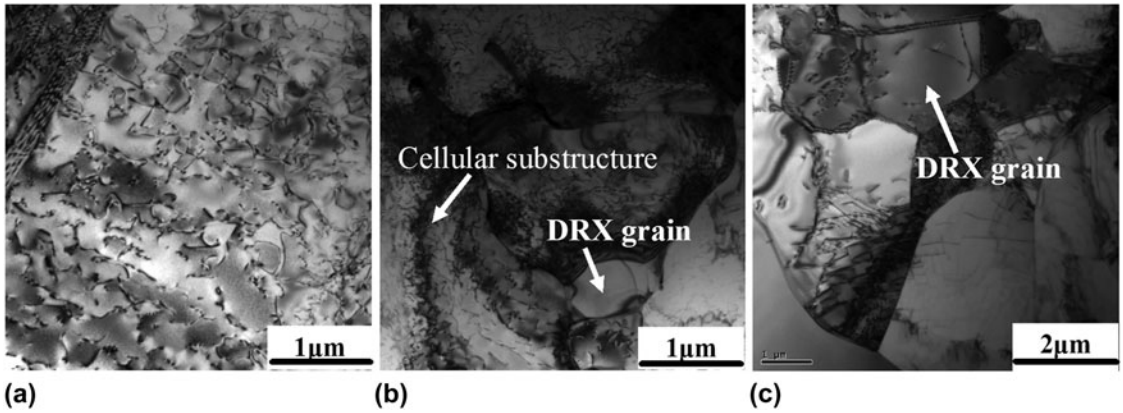



FIG. 7. Matrix microstructures in deformation zones with different strains at 800 °C: (a) about 5%, (b) about 30% and (c) 43% (fracture strain).

aluminium–silicon alloys can act as heterogeneously nucleation substrates for recrystallized α-Al.[42] Hence, recrystallized grains may directly grow on TiC near TiC particles. During the DRX process, new dislocations were generated within DRX grains since the development of deformation depends on dislocation motion [Fig. 7(c)]. Apparently, dynamic recovery and DRX are the flow softening mechanisms in this composite at 800 °C. This result has not been found in published researches in DRTMCs.

Figure 8 exhibits the variation of microstructure in deformation zone with strain at 900 °C. High density of dislocation still can be observed in matrix as stress reached the peak with the strain of about 4% [Fig. 8(a)]. When strain increased to 20%, dislocation density in deformation zone decreased significantly and dislocation tangles almost disappeared, as shown in Fig. 8(b). The high-density dislocations annihilate through dislocation climbing in the subsequent plastic deformation process, which evolved into regular dislocation walls. Comparing Fig. 6(d) with Fig. 8(b), although strain at 700 °C is close to that at 900 °C, the microstructures in the corresponding deformation zones are obviously different. The dislocation density is lower at 700 °C as compared to that at 900 °C, and more importantly, recovered subgrains are formed under this strain at 700 °C [Fig. 6(d)]. Unquestionably, dynamic recovery process was carried out relatively sufficiently at 700 °C. Combining the result in Fig. 4, after macroscopic yielding, the faster decrease in tensile stress with strain reflects that the dislocation annihilation is in a faster rate at 700 °C, whereas dislocation annihilates slowly at 900 °C. Obviously, temperature is not the only factor influencing recovery process during high-temperature tensile deformation. Taking into account that the driving force of recovery is the stored energy in deformed material, the high energy promotes the recovery process more easily. Hence, the distortion energy resulting from dislocation multiplication at 700 °C is higher than that at 900 °C.

With further increase in strain, DRX grains were formed in the deformation zone with diameter of 0.5–2.5 μm, as shown in Fig. 8(c). In the internal of DRX grains, low density dislocation can be observed. Evidently, dislocation slip promotes the continuous plastic deformation of the composite. Furthermore, it is deduced that the dislocation structure in Fig. 8(b) will evolve into recovery subgrains and recovery subgrains develop into DRX grains with the increase of strain from 20% to 60%. When the strain increased to 90%, corresponding to fracture strain, the DRX grains grew up [Fig. 8(d)], leading to the decrease in tensile stress before final failure of the composite at 900 °C. It is obtained that flow softening mechanism at this temperature is similar to that at 800 °C, i.e., dynamic recovery and DRX.

According on the above analysis, temperature has significant influence on microstructure evolution in deformation zones with strain in DRTMCs and their relationship during high-temperature tensile test has been established first in this work, which is the novelty of the present research. Published references have paid more attention on the microstructural evolution during hot deformation in titanium alloys and their composites since their aims are to obtain ideal microstructure for the desired application.[41,43] More importantly, understanding the microstructure evolution during tensile test can provide reasonable explanation for the variation of tensile properties with temperature.

Combining microstructural evolution in deformation zones and tensile stress–strain curves, it is found that the above two are related to each other. The increase of stress with strain often corresponds to the increase in dislocation density during plastic deformation, while the decrease of stress shows the occurrence of dynamic recovery and/or DRX, which lead to matrix softening. Hence, matrix softening is directly reflected in tensile stress–strain curves. The establishment of the relationship between microstructural evolution in deformation zones and tensile stress–strain curves is also the novelty of the present research.

https://doi.org/10.1557/jmr.2016.359 Published online by Cambridge University Press

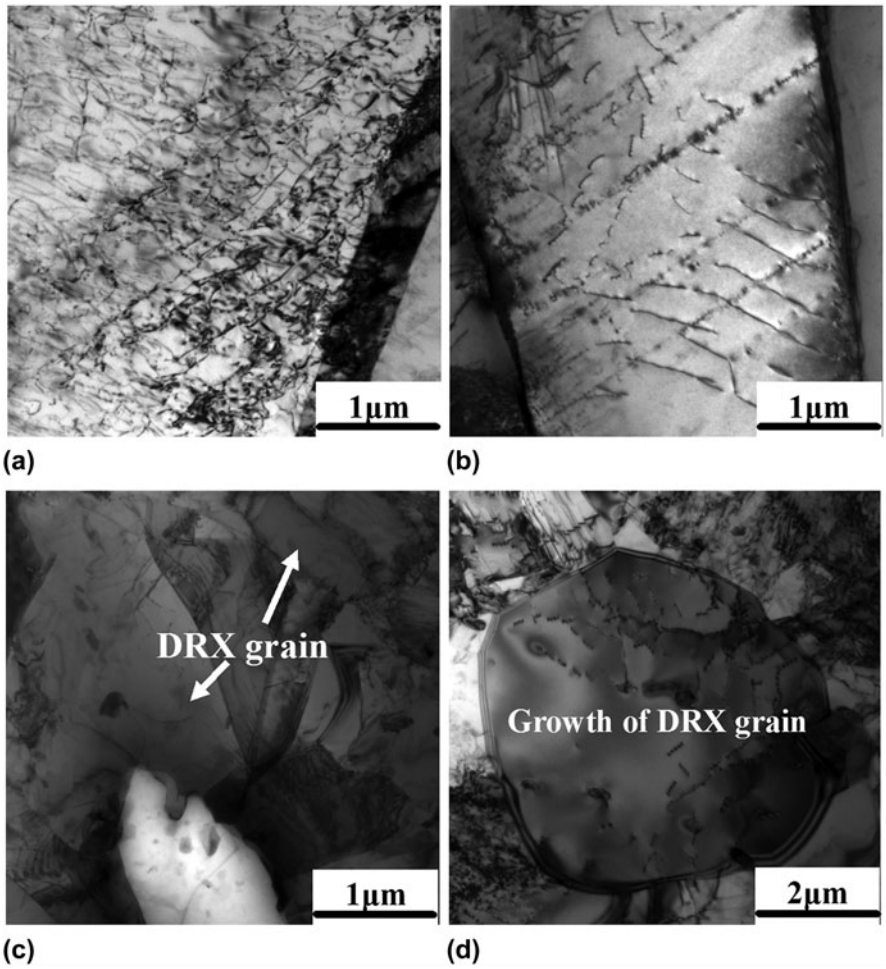



FIG. 8. Matrix microstructure development of the composite in deformation zone at 900 °C under different strains of (a) about 4%, (b) about 20%, (c) about 60% and (d) about 90% (fracture strain).

## IV. CONCLUSION

In this paper, 10 vol%TiC/Ti–6Al–3Sn–3.5Zr–0.4Mo–0.75Nb–0.35Si composite was tested at various temperatures and microstructural evolution in deformation zones has been discussed. The following conclusions can be drawn:

(1) Microstructural evolution in deformation zones with strain showed different trends at different temperatures. Below 600 °C, dislocation density increased with strain over the entire strain range, while at 700 °C, dislocation density increased first and then decreased due to dynamic recovery. Above 800 °C, DRX grains were obtained at high strain.

(2) Below 600 °C, stress increased with the increase of strain whereas above 700 °C, stress decreased with further increase in strain after macroscopic yield.

(3) Microstructural evolution in deformation zones corresponded to the variation of tensile stress–strain characteristics with temperature, reflecting the hardening or softening feature of matrix. As testing temperature exceeded 700 °C, flow softening occurred. At 700 °C, dynamic recovery ascribes to the flow softening, while at 800 °C and 900 °C, flow softening is attributed to dynamic recovery and DRX.

## ACKNOWLEDGMENTS

This work is financially supported by the National Natural Science Foundation of China (Nos. 51601220 and 51671214) and the Science and Technology Planning Project of Jiangsu Province (No. BY2016026-05).

## REFERENCES

1. R. Harichandran and N. Selvakumar: Effect of nano/micro $B_4C$ particles on the mechanical properties of aluminium metal matrix composites fabricated by ultrasonic cavitation-assisted solidification process. *Arch. Civ. Mech. Eng.* **16**, 147 (2016).
2. H.L. Zhang, J.H. Wu, Y. Zhang, J.W. Li, and X.T. Wang: Effect of metal matrix alloying on mechanical strength of diamond particle-reinforced aluminum composites. *J. Mater. Eng. Perform.* **24**, 2556 (2015).

https://doi.org/10.1557/jmr.2016.359 Published online by Cambridge University Press

3. G.Q. Wu, Q.Q. Zhang, X. Yang, Z. Huang, and W. Sha: Effects of particle/matrix interface and strengthening mechanisms on the mechanical properties of metal matrix composites. *Compos. Interfaces* **21**, 415 (2014).
4. H. Abdizadeh and M.A. Baghchesara: Investigation into the mechanical properties and fracture behavior of A356 aluminum alloy-based $ZrO_2$-particle-reinforced metal-matrix composites. *Mech. Compos. Mater.* **49**, 571 (2013).
5. J.Q. Qi, Y. Chang, Y.Z. He, Y.W. Sui, F.X. Wei, Q.K. Meng, and Z.J. Wei: Effect of Zr, Mo and TiC on microstructure and high-temperature tensile strength of cast titanium matrix composites. *Mater. Des.* **99**, 421 (2016).
6. C.J. Zhang, S.Z. Zhang, P. Lin, Z.P. Hou, F.T. Kong, and Y.Y. Chen: Thermomechanical processing of (TiB + TiC)/Ti matrix composites and effects on microstructure and tensile properties. *J. Mater. Res.* **41**, 1244 (2016).
7. M. Zadra and L. Girardini: High-performance, low-cost titanium metal matrix composites. *Mater. Sci. Eng., A* **608**, 155 (2014).
8. X.L. Guo, W.J. Lu, L.Q. Wang, and J.N. Qin: A research on the creep properties of titanium matrix composites rolled with different deformation degrees. *Mater. Des.* **63**, 50 (2014).
9. M. Selva Kumar, P. Chandrasekar, P. Chandramohan, and M. Mohanraj: Characterisation of titanium–titanium boride composites processed by powder metallurgy techniques. *Mater. Charact.* **73**, 43 (2012).
10. J.Q. Lu, J.N. Qin, W.J. Lu, Y. Liu, J.J. Gu, and D. Zhang: In situ preparation of (TiB + TiC + $Nd_2O_3$)/Ti composites by powder metallurgy. *J. Alloys Compd.* **469**, 116 (2009).
11. J.Q. Qi, Y.W. Sui, Y. Chang, Y.Z. He, F.X. Wei, Q.K. Meng, and Z.J. Wei: Superior ductility in as-cast TiC/near-α Ti composite obtained by three-step heat treatment. *Vacuum* **126**, 1–4 (2016).
12. J.Q. Qi, Y.W. Sui, Y. Chang, Y.Z. He, F.X. Wei, Q.K. Meng, and Z.J. Wei: Microstructural characterization and mechanical properties of TiC/near-α Ti composite obtained at slow cooling rate. *Mater. Charact.* **118**, 263 (2016).
13. B. Kaveendran, G.S. Wang, L.J. Huang, L. Geng, Y. Luo, and H.X. Peng: In situ ($Al_3Z_{rp}$ + $Al_2O_{3np}$)/2024Al metal matrix composite with controlled reinforcement architecture fabricated by reaction hot pressing. *Mater. Sci. Eng., A* **583**, 89 (2013).
14. C.J. Zhang, F.T. Kong, S.L. Xiao, E.T. Zhao, L.J. Xu, and Y.Y. Chen: Evolution of microstructure and tensile properties of in situ titanium matrix composites with volume fraction of (TiB plus TiC) reinforcements. *Mater. Sci. Eng., A* **548**, 152 (2012).
15. S.C. Tjong and Y-W. Mai: Processing-structure-property aspects of particulate- and whisker-reinforced titanium matrix composites. *Compos. Sci. Technol.* **68**, 583 (2008).
16. L.J. Huang, L. Geng, H.Y. Xu, and H.X. Peng: In situ TiC particles reinforced Ti6Al4V matrix composite with a network reinforcement architecture. *Mater. Sci. Eng., A* **528**, 2859 (2011).
17. B. Ya, B.W. Zhou, H.S. Yang, B.K. Huang, F. Jia, and X.G. Zhang: Microstructure and mechanical properties of in situ casting TiC/Ti6Al4V composites through adding multi-walled carbon nanotubes. *J. Alloys Compd.* **637**, 456 (2015).
18. H. Rastegari and S.M. Abbasi: Producing Ti–6Al–4V/TiC composite with superior properties by adding boron and thermo-mechanical processing. *Mater. Sci. Eng., A* **564**, 473 (2013).
19. P. Nandwana, J.Y. Hwang, M.Y. Koo, J. Tiley, S.H. Hong, and R. Banerjee: Formation of equiaxed alpha and titanium nitride precipitates in spark plasma sintered TiB/Ti–6Al–4V composites. *Mater. Lett.* **83**, 202 (2012).
20. L.J. Huang, L. Geng, H.X. Peng, and B. Kaveendran: High temperature tensile properties of in situ $TiB_w$/Ti6Al4V composites with a novel network reinforcement architecture. *Mater. Sci. Eng., A* **534**, 688 (2012).
21. H.W. Wang, J.Q. Qi, C.M. Zou, D.D. Zhu, and Z.J. Wei: High-temperature tensile strengths of in situ synthesized TiC/Ti-alloy composites. *Mater. Sci. Eng., A* **545**, 209 (2012).
22. D. Liu, S.Q. Zhang, A. Li, and H.M. Wang: High temperature mechanical properties of a laser melting deposited TiC/TA15 titanium matrix composite. *J. Alloys Compd.* **496**, 189 (2010).
23. L. Xiao, W.J. Lu, J.N. Qin, D. Zhang, M.M. Wang, F. Zhu, and B. Ji: High-temperature tensile properties of in situ-synthesized titanium matrix composites with strong dependence on strain rates. *J. Mater. Res.* **233**, 3066 (2008).
24. C. Badini, G. Ubertalli, D. Puppo, and P. Fino: High temperature behaviour of a Ti–6Al–4V/TiCp composite processed by BE-CIP-HIP method. *J. Mater. Sci.* **35**, 3903 (2000).
25. J.Q. Lu, J.N. Qin, W.J. Lu, Y.F. Chen, D. Zhang, and H.L. Hou: Hot deformation behavior and microstructure evaluation of hydrogenated Ti–6Al–4V matrix composite. *Int. J. Hydrogen Energ.* **349**, 266 (2009).
26. Y.Q. Ning, B.C. Xie, H.Q. Liang, H. Li, X.M. Yang, and H.Z. Guo: Dynamic softening behavior of TC18 titanium alloy during hot deformation. *Mater. Des.* **71**, 68 (2015).
27. C. Poletti, L. Germain, F. Warchomicka, M. Dikovits, and S. Mitsche: Unified description of the softening behavior of beta-metastable and alpha plus beta titanium alloys during hot deformation. *Mater. Sci. Eng., A* **651**, 280 (2016).
28. A. Majorell, S. Srivatsa, and R.C. Picu: Mechanical behavior of Ti–6Al–4V at high and moderate temperatures—Part I: Experimental results. *Mater. Sci. Eng., A* **326**, 297 (2002).
29. J.Q. Qi, H.W. Wang, C.M. Zou, W.Q. Wei, and Z.J. Wei: Temperature dependence of fracture behavior of in situ synthesized TiC/Ti-alloy matrix composite. *Mater. Sci. Eng., A* **528**, 7669 (2011).
30. A.A.M. da Silva, J.F. dos Santos, and T.R. Strohaecker: Microstructural and mechanical characterisation of a Ti6Al4V/TiC/10p composite processed by the BE-CHIP method. *Compos. Sci. Technol.* **65**, 1749 (2005).
31. J.H. Zhu, P.K. Liaw, J.M. Corum, and H.E. McCoy: High-temperature mechanical behavior of Ti–6Al–4V alloy and TiCp/Ti–GAl–4V composite. *Metall. Mater. Trans. A* **30**, 1569 (1999).
32. C.J. Boehlert, C.J. Cowen, S. Tamirisakandala, D.J. McEldowney, and D.B. Miracle: In situ scanning electron microscopy observations of tensile deformation in a boron-modified Ti–6Al–4V alloy. *Scr. Mater.* **55**, 465 (2006).
33. Z.F. Yang, W.J. Lu, J.N. Qin, and D. Zhang: Microstructure and tensile properties of in situ synthesized (TiB + TiC + $Nd_2O_3$)/Ti-alloy composites at elevated temperature. *Mater. Sci. Eng., A* **425**, 185 (2006).
34. B. Liu, Y.P. Li, H. Matsumoto, Y.B. Liu, Y. Liu, H.P. Tang, and A. Chiba: Thermomechanical response of particulate-reinforced powder metallurgy titanium matrix composites—A study using processing map. *Mater. Sci. Eng., A* **527**(18–19), 4733 (2010).
35. W.W. Peng, W.D. Zeng, Q.J. Wang, Q.Y. Zhao, and H.G. Yu: Effect of processing parameters on hot deformation behavior and microstructural evolution during hot compression of as-cast Ti60 titanium alloy. *Mater. Sci. Eng., A* **593**, 16 (2014).
36. Y.Y. Zong, D.B. Shan, M. Xu, and Y. Lv: Flow softening and microstructural evolution of TC11 titanium alloy during hot deformation. *J. Mater. Process. Technol.* **209**, 1988 (2009).
37. Y. Liu, J.C. Zhu, Y. Wang, and J.J. Zhan: Hot compressive deformation behavior and microstructure evolution of Ti–6Al–2Zr–1Mo–1Valloy at 1073 K. *Mater. Sci. Eng., A* **490**, 113 (2008).
38. Y.Q. Ning, X. Luo, H.Q. Liang, H.Z. Guo, J.L. Zhang, and K. Tan: Competition between dynamic recovery and recrystallization


https://doi.org/10.1557/jmr.2016.359 Published online by Cambridge University Press

during hot deformation for TC18 titanium alloy. *Mater. Sci. Eng., A* **635**, 77 (2015).
39. F.T. Furuhara, B. Poorganji, H. Abe, and T. Maki: Dynamic recovery and recrystallization in titanium alloys by hot deformation. *JOM* **59**, 64 (2007).
40. F.J. Humphreys and M. Hatherly: *Recrystallization and Related Annealing Phenomena*, 2nd ed. (Elsevier, Oxford, 2004); p. 53.
41. B. Wang, L.J. Huang, B.X. Liu, L. Geng, and H.T. Hu: Effects of deformation conditions on the microstructure and substructure evolution of $TiB_w$/Ti60 composite with network structure. *Mater. Sci. Eng., A* **627**, 316 (2015).
42. H.M. Chan and F.J. Humphreys: The recrystallisation of aluminium–silicon alloys containing a bimodal particle distribution. *Acta Metall.* **32**(2), 235 (1984).
43. S. Roy and S. Suwas: The influence of temperature and strain rate on the deformation response and microstructural evolution during hot compression of a titanium alloy Ti–6Al–4V–0.1B. *J. Alloys Compd.* **548**, 110 (2013).

https://doi.org/10.1557/jmr.2016.359 Published online by Cambridge University Press